EPJ Web of Conferences **21**, 08003 (2012)
DOI: 10.1051/epjconf/20122108003

Monte Carlo Hauser-Feshbach Modeling of Prompt Fission Neutrons and Gamma Rays

Patrick Talou[1,a], Bjorn Becker[2], Toshihiko Kawano[1], and Yaron Danon[2]

[1] T-2, Nuclear Theory Group, Los Alamos National Laboratory, Los Alamos, NM, USA
[2] Gaertner LINAC Laboratory, Rensselaer Polytechnic Institute, New York 12180, USA

Abstract. The decay of fission fragments is studied through Monte Carlo Hauser-Feshbach model calculations taking into account the competition between the emissions of prompt fission neutrons and gamma rays. The importance of initial excitation energy and spin distribution in the primary light and heavy fragments is demonstrated through comparison with experimental data. Excitation energy sorting mechanisms at scission are discussed in the light of these advanced simulations. Preliminary results on prompt fission gamma rays are also reported.

1 Introduction

Prompt fission neutrons and gamma rays constitute the first signature of post-scission physics. They indicate not only how much total energy is released in fission but also inform about the intricate physical processes at work near the point of separation of the two fragments. New theoretical and experimental tools have been developed recently in order to study them in a more detailed manner than in the past, shedding some light on distributions and correlations of quantities for which we knew only about averages. On the theoretical side, Monte Carlo simulations of the fission fragment evaporation stage have been carried out by several groups [1–4]. They all share the same techniques based on a Weisskopf evaporation spectrum for the emission of prompt neutrons. Gamma rays have been considered only as a by-product of the final stage of the decay where no more neutron could be emitted. More recently, Litaize and Serot [3] have introduced a slightly more accurate description of the neutron−gamma competition, albeit in a phenomenological correction to the Weisskopf-type approach only.

In the present publication, we discuss the use of Monte Carlo Hauser-Feshbach (MCHF) simulations to study the emission of prompt neutrons and gamma rays from excited primary fission fragments. The Hauser-Feshbach statistical reaction theory provides a more accurate framework for describing the competition between neutrons and gamma rays than the simpler Weisskopf approach. The MCHF technique is discussed in detail by Kawano *et al.* at this Conference [5], and only a brief description will be included here.

MCHF calculations of fission fragment decay rely on more parameters than simpler Weisskopf calculations, and are definitely more CPU intensive as they require a calculation of neutron and gamma emission probabilities for each decay step, while ensuring angular momentum conservation rules. In particular the initial spin distribution in the fission fragments has to be known to a certain accuracy, as it impacts the competition between neutrons and gamma rays significantly.

In addition, the question of excitation energy sharing among the two fragments is more relevant than ever. Recent noticeable efforts by Schmidt and Jurado [6,7] have shed some light on an energy sorting mechanism for low excitation energies. While this work dealt with intrinsic excitation energy

[a] e-mail: talou@lanl.gov

available at scission, the estimation of the remaining deformation and collective energies locked at scission, but later released in the individual fragments as intrinsic excitation energy, remains unclear.

The present paper will address those questions. Section 2.1 introduces the MCHF technique, followed by a discussion on the choice of model input parameters present in MCHF calculations. More specifically, section 2.3 discusses the energy sharing mechanisms at work at scission. Numerical results are then presented and discussed in the case of n_{th}+^{239}Pu and ^{252}Cf (sf). Special emphasis is placed on the distinction between MCHF and Weisskopf-based results and on the role played by the initial spin distribution in the primary fragments.

2 Model Overview

2.1 Monte Carlo Hauser-Feshbach

The Hauser-Feshbach statistical model [8] is used to compute the decay probabilities of the excited fragments by either neutron or gamma-ray emission. A Monte Carlo Hauser-Feshbach (MCHF) code, CGM, was implemented [5] and used in the present work. A significant advantage of the Monte Carlo technique over more traditional deterministic approaches is that it provides distributions and correlations of calculated quantities rather directly. The extraction of the same quantities in the deterministic approach would be both cumbersome and approximate at best. The CGM code was combined with our previous FFD code that simulates the decay of fission fragments for a range of compound nuclei, using our best estimates of the initial fission fragment yields, and model parameter input libraries such as the Reference Input Parameter Library RIPL-3 [9].

The probabilities for gamma-ray and neutron emissions are given by

$$P(\epsilon_\gamma)dE \propto T_\gamma(\epsilon_\gamma)\rho(Z,A,E-\epsilon_\gamma), \tag{1}$$

and

$$P(\epsilon_n)dE \propto T_n(\epsilon_n)\rho(Z,A-1,E-\epsilon_n-S_n), \tag{2}$$

where $T_{\gamma,n}$ are energy-dependent transmission coefficients, $\rho(A,Z,E)$ is the level density in the nucleus (A,Z) at excitation energy E, and S_n is the neutron separation energy. The neutron transmission coefficients are calculated exactly at each time step using an optical model potential, and the gamma-ray transmission coefficient is obtained in the gamma-ray strength function formalism, with default parameters taken from the RIPL-3 database [9].

The level density $\rho(E)$ is represented in the Gilbert-Cameron formalism [10], with a constant temperature model at the lowest excitation energies and a Fermi gas representation at higher energies, taking into account the washing-out of shell effects with increasing excitation energy [11]. Here again, the RIPL-3 systematics for the level density parameters were used.

2.2 Model Input Parameters

Performing MCHF calculations for fission fragments requires to know various quantities. The starting point is the fission fragment distributions in mass, charge, excitation energy, spin and parity. Several theoretical efforts are underway to address this question [12–14], but remain too imprecise at this stage to be used in our calculations. So one has to rely on experimental data and systematics to obtain the pre-neutron emission fragment yields $Y(A,Z,TKE)$. This information is never complete, and fragmentary data have to be assembled to generate this distribution. An example is shown in Fig. 1 where the fission fragment yields obtained in the thermal neutron-induced fission of ^{239}Pu have been estimated (see Ref. [4] for more details).

For a given fragmentation (A_l,Z_l)+(A_h,Z_h) and total kinetic energy TKE, the total excitation energy TXE is known, as long as nuclear masses are relatively well predicted. Those masses are taken from the Audi, Wapstra and Thibault tables [15].

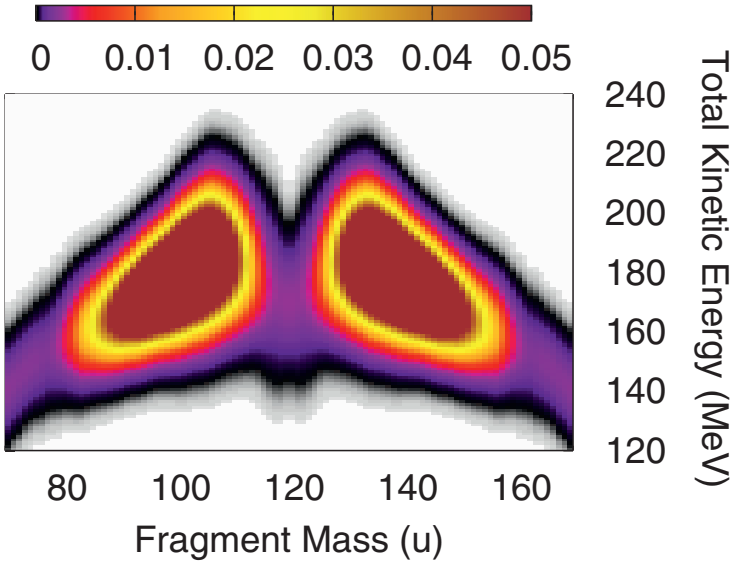

Fig. 1. Fission fragment yields in the thermal neutron-induced fission of ^{239}Pu, as obtained and explained at length in Ref. [4].

The sharing of TXE between the light and heavy fragments is not known however, and is discussed at some length in Section 2.3.

Various experimental studies [16–18] have addressed the question of the initial spin distribution in the fission fragments shortly after scission. This is an important ingredient in MCHF calculations as it strongly impacts the competition between neutron and gamma-ray emissions. Experimentally, this information is usually extracted from measured isomeric ratios [17,18]. In those preliminary studies, we have tested various hypotheses for the initial spin distributions, as will be discussed below.

2.3 Excitation Energy Sharing near Scission

The total excitation energy (TXE) available in the fission process for a specific fragmentation can be inferred from calculated masses and experimental total kinetic energy (TKE) values as

$$\begin{aligned} TXE &= Q_f + E_n^{inc} + B_n(Z_c, A_c) - TXE \\ &= M_n(Z_l, A_l) + M_n(Z_h, A_h) - M_n(Z_c, A_c) \\ &\quad + E_n^{inc} + B_n(Z_c, A_c) - TKE, \end{aligned} \tag{3}$$

where E_n^{inc} is the incident neutron energy and B_n the neutron binding energy in the compound nucleus. The sharing of TXE between the light and heavy fragments remains an important and open question. Schmidt and Jurado have recently proposed [6,7] an energy sorting mechanism based on thermal equilibrium at scission, which leads to a transfer of energy from the "hot" fragment to the "cold" one. This scenario is based on the known behavior of nuclear level densities at the lowest excitation energies, which are better represented by a constant-temperature formalism than by a Fermi gas expression. This is at the core of the Gilbert-Cameron level density representation [10] that is used in all fission fragment decay codes. Since a general trend for the nuclear temperature is to decrease with A [19,20], the light fragment would in general be hotter than its heavy partner. This result can be significantly modified however by the proximity of the fragments to shell closures.

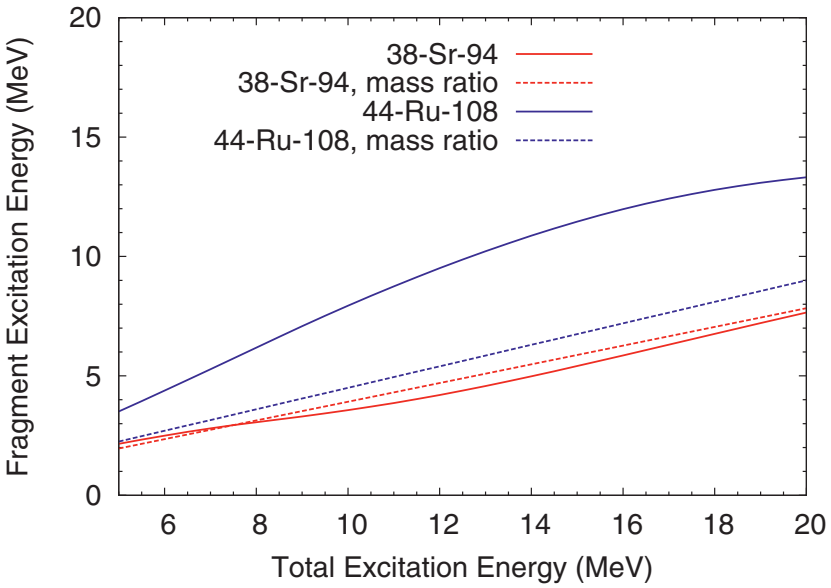

Fig. 2. The energy sorting mechanism proposed by Schmidt and Jurado [7] is used to compute the excitation energy in the light fragment as a function of the total excitation energy available at scission in the fission of ^{240}Pu*. The original case presented in [7] corresponds to a light fragment ^{94}Sr, as shown in red here. In this case, the temperature in the light fragment is slightly higher than its heavy counterpart, and more excitation energy is carried away by the heavy fragment, compared to a simple mass ratio formula (dashed lines). However, an opposite scenario is seen in the case of ^{108}Ru for which the heavy counterpart is the doubly magic nucleus ^{132}Sn.

Implementing the energy sorting mechanism proposed by Schmidt and Jurado [7], we calculated the nuclear temperatures and corresponding intrinsic excitation energies of the fission fragments produced in the thermal neutron-induced fission of ^{239}Pu. Following [7], the average excitation energy in the light fragment is given by

$$\langle E_l \rangle = \frac{\int_0^{E^*_{int}} E_l \rho_l(E_l)\rho_h(E^*_{int} - E_l)dE_l}{\int_0^{E^*_{int}} \rho_l(E_l)\rho_h(E^*_{int} - E_l)dE_l}, \tag{4}$$

where $\rho_{l,h}$ are the level densities in the light and heavy fragment respectively, and E^*_{int} is the total intrinsic excitation energy available in the composite fissioning system. The most probable value of E_l occurs when the maximum entropy is reached. We have performed this calculation in the case of thermal neutron-induced fission of ^{239}Pu. The result is shown in Fig. 2 for a couple of different fragmentations. We reproduce the result obtained in [7] for ^{94}Sr, i.e., the light fragment gets less excitation energy, compared to what would be obtained with a simple mass ratio formula, due to a higher temperature in the constant-temperature regime of the Gilbert-Cameron representation.

However, this tendency is strongly reversed in the case of ^{108}Ru for which its heavy partner is the doubly magic nucleus ^{132}Sn. While the temperature is even difficult to define in this case due to this scarcity of discrete levels in ^{132}Sn, a large portion of the total energy then goes into the light fragment. While the importance of shell effects in inverting the light-to-heavy fragment energy sorting mechanism was mentioned in [7], the conclusions regarding the evolution of neutron emission as a function of total excitation energy assumed that this inversion is more the exception than the rule. Of course, this conclusion depends on the specific pairs of fragments produced in the reaction.

To study this mechanism in light of prompt fission neutron data, we performed energy sorting calculations for all fragments involved in the reaction n_{th}+^{239}Pu and weighted the results by the fission fragment yields $Y(A, Z, TXE)$ to obtain the temperature ratio $R_T = T_l/T_h$ as a function of the heavy fragment mass. To obtain this result, we consider the extreme situation in which all of TXE is available

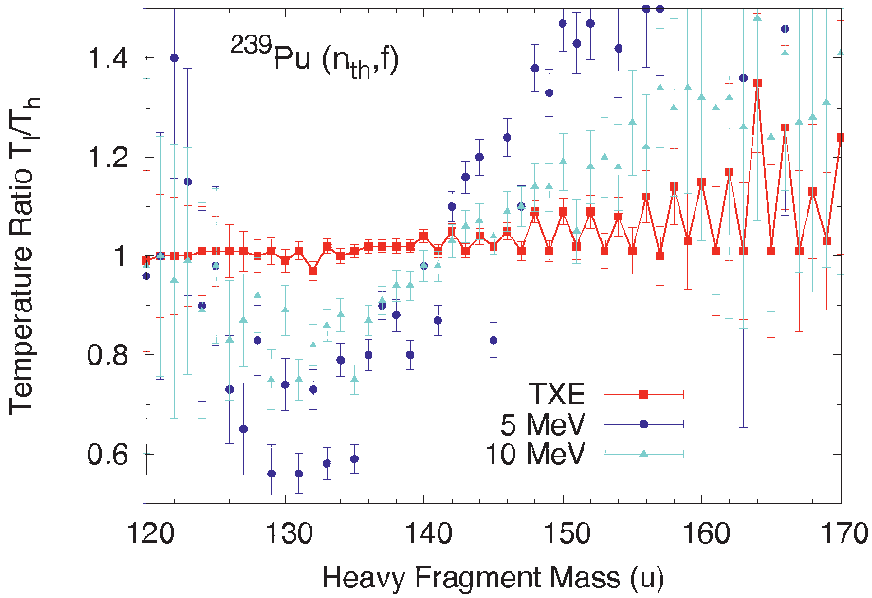

Fig. 3. The average ratio of the temperatures in the light (T_l) and heavy (T_h) fragments is plotted as a function of the heavy fragment mass, for several excitation energies. At low excitation energies, the effect of the temperature sorting mechanism discussed in [6] is clearly visible, but is strongly hampered at higher excitation energies. Odd-even effects are also clearly visible on this figure, as only one charge Z per fragment mass was used in this calculation.

at scission. The result is shown in Fig. 3. The ratio R_T is indeed larger than 1.0 for most fragmentations, and increases with mass asymmetry. This ratio remains less than 1.1 for most values however. This result is in stark contrast with the empirical result shown in Fig. 10 of Ref. [4], inferred from experimental values on the ratio $\overline{\nu}_l/\overline{\nu}_h(A_h)$. In fact, most of this behavior can be readily explained by the proximity of spherical closed shells as already mentioned in [4]. Of course, TXE is usually not fully available at scission, e.g., stored in deformation phase-space, and the effect of the energy sorting mechanism described above could still strongly influence the intrinsic excitation energy sharing. However, its influence on the total excitation energy available for the emission of neutrons and gamma rays would then be smaller.

3 Results

3.1 Monte Carlo Weisskopf

It was shown in [4] that the average prompt fission neutron multiplicity (PFNM) could be calculated very accurately in the case of thermal and fast neutron-induced fission of ^{239}Pu. The calculated average thermal PFNM is $\overline{\nu}_c$=2.871, in excellent agreement with other evaluated results, $\overline{\nu}$=2.8725 in the ENDF/B-VII.0 library, and $\overline{\nu}$ = 2.8771 ± 0.0047 for the evaluation by the IAEA Standards working group [21]. For 500 keV incident neutrons, the calculated result obtained by assuming similar initial fission fragment yields and adding 0.5 MeV to the total excitation energy was 2.932 to compare with 2.939 in the ENDF/B-VII.0 evaluation.

The PFNS was calculated using two different assumptions for the R_T parameter: (i) a constant value of 1.1; (ii) a mass-dependent ratio R_T(A) extracted from experiments to reproduce the observed ratio of neutron mulitplicities $\overline{\nu}_l/\overline{\nu}_h$(A). The results are shown in Fig. 4, and compared with the ENDF/B-VII.0 spectrum, as well as selected experimental data sets for incident neutron energies less than 0.5 MeV. The Monte Carlo results reproduce the experimental data very well in the most accurate outgoing energy range, and follows the ENDF/B-VII.0 values there fairly well. Below 500 keV and above 8

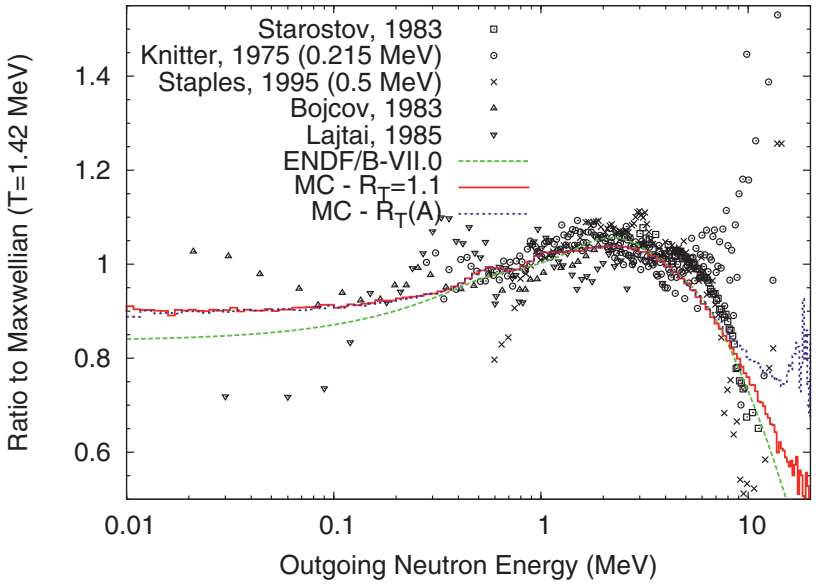

Fig. 4. The calculated prompt fission neutron spectrum for the thermal neutron-induced fission reaction on ^{239}Pu is shown as a ratio to a Maxwellian with temperature T=1.42 MeV, and compared to selected experimental data sets. Two options for the Monte Carlo calculations are shown. See text for details.

MeV, the Monte Carlo results deviate from the ENDF/B-VII.0 evaluation, which is based on Madland-Nix model calculations. The two Monte Carlo results are very similar except above 8 MeV, where the one obtained with R_T(A) is harder. As was discussed in [4], this result leads to better $\overline{\nu}_{calc}$(A) but worsens $\overline{\epsilon}_{calc}$(A), and should only be viewed as a sensitivity test for the Monte Carlo simulations. Note that the Monte Carlo calculated PFNS lie well within the current experimental as well as evaluated uncertainties [22].

Figure 5 shows the quantity $-d\overline{\nu}/dTKE$ as a function of the fragment mass. A linear representation of the functions $\overline{\nu} = f$(TKE) was assumed for all fragment masses. While this assumption is well verified in most cases, the fits were not as clean for some fragmentations and can lead to fluctuations in the calculated points shown in Fig. 5. The particular behavior of $-d\overline{\nu}/dTKE$ as a function of the fragment mass can be explained again by the proximity of the fragments to a spherical shell closure.

Other quantities of interest have been calculated and are discussed at some length in [4].

3.2 Monte Carlo Hauser-Feshbach

In all previous studies (e.g. [2–4]), the de-excitation of the fission fragments has been studied by assuming a Weisskopf-type spectrum for the neutron emission, and prompt gamma rays were not studied directly, but only inferred from the excitation energy left in the residual fission product under which no more neutron could be emitted. This energy limit was somewhat arbitrarily chosen above the neutron binding energy to grossly simulate the neutron−gamma competition. In MCHF calculations, this extra parameter disappears as the competition is accounted for according to the probabilities of gamma and neutron emissions (cf. Eqs. 1 and 2).

Figure 6 illustrates the competition between neutrons and gamma rays. For low spin values, the ratio Γ_γ/Γ_n is nearly a step function with a transition from 0 to 1 at excitation energies close to the neutron separation energy. Higher spin values increase the probability of gamma emission at the expense of neutron emission. The transition also spans a wider energy range.

Experimental studies [17, 18] show some evidence that fission fragments carry relatively high spin values after scission. Using an initial spin population centered around the ground-state value, i.e.,

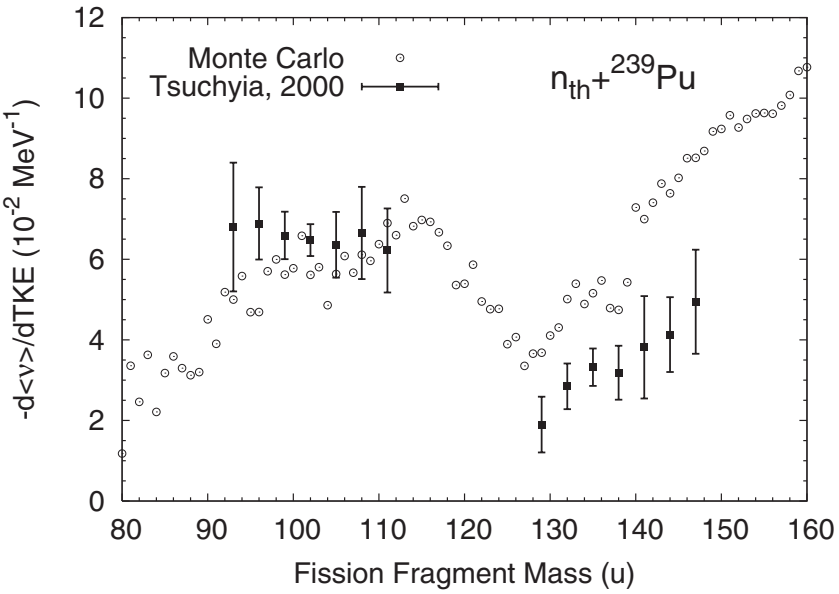

Fig. 5. The variation of $\overline{\nu}$ with TKE is shown as a function of the fragment mass. The calculated points were obtained by fitting the calculated functions $\overline{\nu} = f(\text{TKE})$ with straight lines. This assumption was well verified in most cases, but not all.

with low-spin values, MCHF calculations predict too many prompt neutrons at the expense of prompt gamma rays. Only if higher spin values are included does the prompt neutron multiplicity tends to the experimental values, while increasing the number of prompt gamma rays. Therefore our preliminary results indicate that $\overline{\nu}_p$ can only be reproduced with MCHF calculations if part of the gamma rays are emitted prior to reaching the neutron separation energy.

Following [23], we have assumed that the spin population can be represented as

$$P(J) \propto (2J+1)\exp\left[-\frac{(J+1/2)^2}{B^2}\right], \tag{5}$$

where $B \sim J_{rms}$. This quantity is related to the moment of inertia of the fission fragment at the excitation energy it is formed at. In these preliminary calculations, we are interested in studying the sensitivity of the results to a particular choice of B. As mentioned earlier, if B is too small, then the number of neutrons emitted is overestimated. On the other hand, if its value is too high, the gamma multiplicity tends to be too high also, and the average gamma-ray energy $\langle E_\gamma \rangle$ is lower than experimental data suggest. Considering a constant, mass-independent value for B, reasonable values range from 6 to 10$\hbar$. The assumption that B does not depend on the fragment is obviously a gross simplification at this stage.

The prompt fission gamma spectrum (PFGS) calculated for n_{th}+^{239}Pu using a constant value of $B = 7\hbar$ is shown in Fig. 7 with the ENDF/B-VII.0 spectrum, which is directly taken from the experimental data of Verbinski *et al.* [24]. The agreement between calculation and experiment is rather good.

A similar result was obtained for the ^{252}Cf (sf) and is shown in Fig. 8. In this case, B was chosen as 9$\hbar$. The calculated prompt fission gamma ray multiplicity distribution $P(N_\gamma)$ is compared to the Brunson's model [25] in Fig. 9. Our preliminary results are reasonable, but slightly underestimates the average gamma-ray multiplicity. Note that our results are very sensitive to the specific gamma-ray energy threshold, and should be tuned to the experimental value, i.e., 140 keV in the present case.

As mentioned earlier, the initial spin population in a primary fragment is very likely linked to its excitation energy and its moment of inertia. Therefore a mass-independent and energy-independent value for B is most certainly wrong. More exclusive data as a function of the fragment mass can cer-

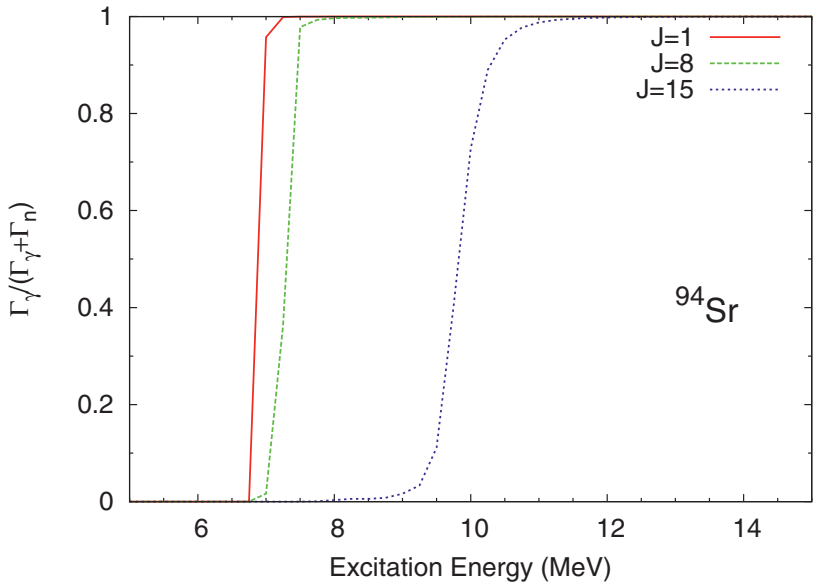

Fig. 6. The gamma-ray emission probability $P_\gamma = \Gamma_\gamma/(\Gamma_\gamma + \Gamma_n)$ is plotted as a function of the excitation energy for different spin values. For low spins, the transition from 0 to 1 is very close to a step function and occurs near the neutron separation energy. For higher spin values, e.g., J=15, the transition occurs at higher excitation energies and spans a wider energy range.

tainly help decide about this question. Figure 10 shows the calculated average prompt fission gamma-ray multiplicity as a function of the fragment mass, and compared to two different data sets. Striking differences appear between those two data sets, as one shows a saw-tooth behavior similar to what is observed for $\overline{\nu}$(A), while the other depicts a function almost constant across the fragment mass axis. New measurements would be of great interest to resolve this question.

4 Conclusion

In this contribution, we have presented for the first time results of Monte Carlo Hauser-Feshbach simulations of the decay of excited primary fission fragments. In contrast with earlier calculations that assumed a simpler Weisskopf evaporation spectrum for the prompt neutrons and did not compute compute prompt gamma rays, full MCHF calculations describe the competition between neutrons and gamma rays in a consistent framework. They require an important additional information regarding the initial spin distribution of the primary fragments, and the preliminary results presented here show that some of the results can be very sensitive to this input. Those results also show that the predicted prompt fission gamma spectrum reproduces fairly well the (scarce) experimental data.

From these calculations, it clearly appears that renewed experimental efforts in studying both prompt fission neutrons as well as gamma rays should be a priority in order to better constrain the models that have been developed, and which still require input parameters that cannot be established by theory just yet.

The question of the sharing of the total excitation energy at scission was also discussed. In particular, the energy sorting mechanism introduced by Schmidt and Jurado [6] was studied. While the effect exists, it is strongly damped in the case of fission for two main reasons: (i) the initial excitation energies in the primary fragments are relatively high, and therefore the constant-temperature regime of the level densities may not be valid anymore; it should be said however that large uncertainties remain regarding the level densities in those fragments; (ii) the proximity of the fragments to spherical shell

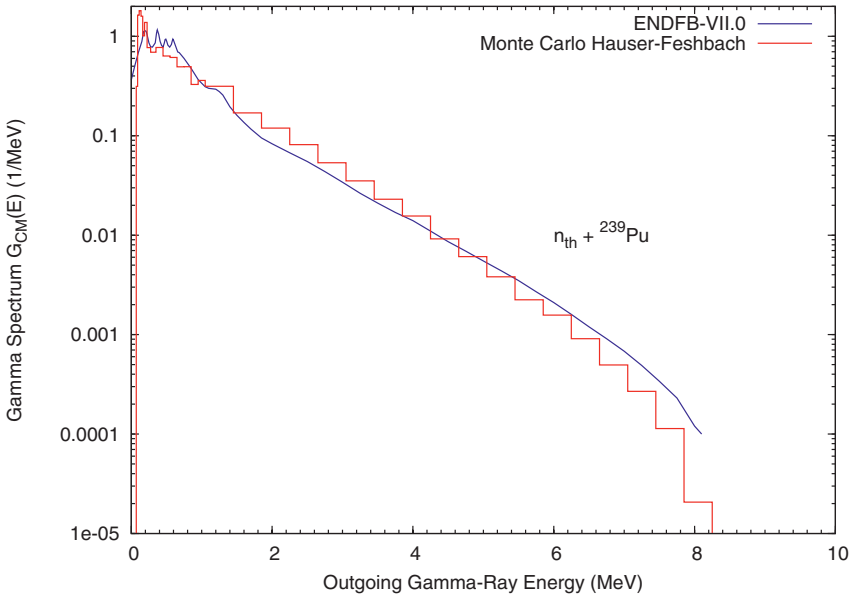

Fig. 7. The prompt fission gamma spectrum (PFGS) calculated for the reaction ^{239}Pu (n_{th}, f) is compared to the ENDF/B-VII.0 evaluation, which is directly taken from the experimental data by Verbinski *et al.* [24].

closures tend to invert the temperature ratio between the light and heavy fragments, thereby reducing the impact as if all light fragments had a higher temperature than their heavy counterparts.

Acknowledgements

We would like to thank M.B. Chadwick, D.G. Madland, J. Lestone, P. Möller, A.J. Sierk, and R.C. Haight for stimulating discussions.

References

1. S. Lemaire, P. Talou, T. Kawano, M.B. Chadwick, and D.G. Madland, Phys. Rev. C**72**, (2005) 024601.
2. R. Vogt, J. Randrup, J. Pruet, and W. Younes, Phys. Rev. C**80**, (2009) 044611.
3. O. Litaize and O. Serot, Phys. Rev. C**82**, (2010) 054616.
4. P. Talou, B. Becker, T. Kawano, M.B. Chadwick, and Y. Danon, Phys. Rev. C**83**, (2011) 064612.
5. T. Kawano, P. Talou and M.B. Chadwick, *this Conference*.
6. K.-H. Schmidt and B. Jurado, Phys. Rev. Lett. **104**, (2010) 212501.
7. K.H. Schmidt and B. Jurado, Phys. Rev. C**83**, (2011) 061601(R).
8. W. Hauser and H. Feshbach, Phys. Rev. **87**, (1952) 366.
9. R. Capote, M. Herman *et al.*P. Oblozinsky, P.G. Young, S. Goriely, T. Belgya, A.V. Ignatyuk, A.J. Koning, S. Hilaire, V.A. Plujko, M. Avrigeanu, O. Bersillon, M.B. Chadwick, T. Fukahori, Zhigang Ge, Yinlu Han, S. Kailas, J. Kopecky, V.M. Maslov, G. Reffo, M. Sin, E.Sh. Soukhovitskii and P. Talou, Nuclear Data Sheets **110**, (2009) 3107.
10. A. Gilbert and A.G.W. Cameron, Can. J. Phys. **43**, (1965) 1446.
11. A.V. Ignatyuk, K.K. Istekov, and G.N. Smirenkin, Sov. J. Nucl. Phys. **29**, (1979) 450.
12. J. Randrup and P. Möller, Phys. Rev. Lett. **106**, (2011) 132503.
13. W. Younes and D. Gogny, Phys. Rev. Lett. **107**, (2011) 132501.

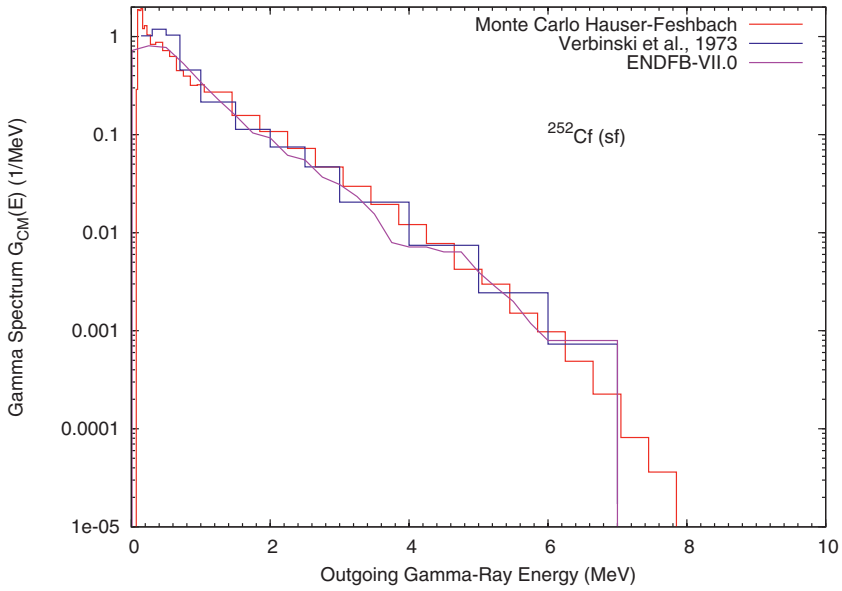

Fig. 8. Same as Fig. 7 for the ^{252}Cf spontaneous fission.

14. N. Dubray, H. Goutte, and J.-P. Delaroche. Phys. Rev. C**77**, (2008) 014310.
15. G. Audi, A.H. Wapstra, and C. Thibault, Nucl. Phys. **A729**, (2003) 337.
16. F. Pleasonton, Nucl. Phys. **A213**, (1973) 413.
17. J.B. Wilhelmy, E. Cheifetz, R.C. Jared, S.G. Thompson, and H.R. Bowman, Phys. Rev. C**5**, (1972) 2041.
18. H. Naik, S.P. Dange, and R.J. Singh, Phys. Rev. C**71**, (2005) 014304.
19. T. von Egidy and D. Bucurescu, Phys. Rev. C**72**, (2005) 044311.
20. T. Kawano, S. Chiba, and H. Koura, J. Nucl. Sci. Tech. **43**, (2006) 1.
21. A.D. Carlson, V.G. Pronyaev, D.L. Smith, N.M. Larson, C. Zhenpeng, G.M. Hale, F.-J. Hambsch, E.V. Gai, S.Y. Oh, S.A. Badikov, T. Kawano, H.M. Hofmann, H. Vonach, and S. Tagesen, Nuclear Data Sheets **110**, (2009) 3215.
22. P. Talou, T. Kawano, D.G. Madland, A.C. Kahler, D.K. Parsons, M.C. White, R.C. Little and M.B. Chadwick, Nucl. Sci. Eng. **166**, (2010) 254.
23. D. De Frenne, in *The Nuclear Fission Process*, Ed. C. Wagemans, CRC Press, Boca Raton, (1991) 475.
24. V.V. Verbinski, H. Weber, and R.E. Sund, Phys. Rev. C**7**, (1973) 1173.
25. T.E. Valentine, ORNL Technical Report, ORNL/TM-1999/300 (1999).
26. *"Untersuchung der spontanen Spaltung von 252Cf am Darmstadt-Heidelberger-Kristallkugel-Spektrometer,"* Max Planck Institute for Nuclear Physics, Report H - V15, in German (1989).

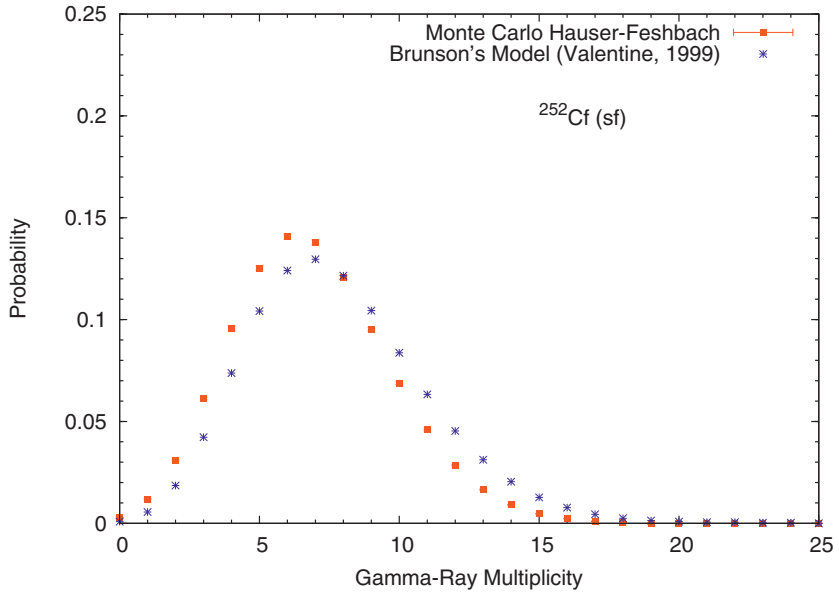

Fig. 9. The prompt fission gamma-ray multiplicity distribution $P(N_\gamma)$ is calculated for the ^{252}Cf spontaneous fission, and compared to two statistical models used by Valentine [25].

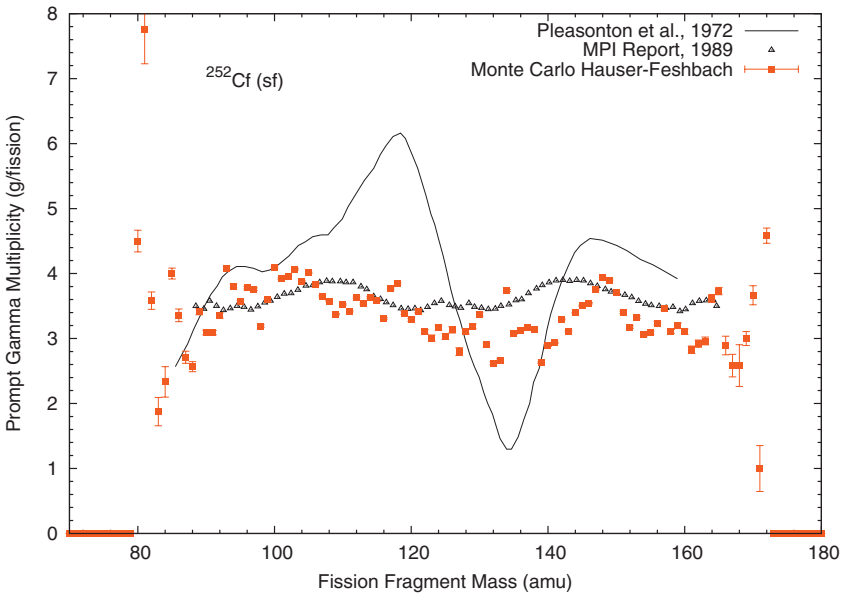

Fig. 10. The calculated average prompt fission neutron multiplicity is plotted as a function of the fragment mass, and compared to experimental data by Pleasonton *et al.* and MPI [26].